

AD 679905

NOLTR 68-114

THE CAVITY AFTER VERTICAL WATER ENTRY

NOL

12 JULY 1968

JAN 2 1969

UNITED STATES NAVAL ORDNANCE LABORATORY, WHITE OAK, MARYLAND

NOLTR 68-114

This document has been approved for public  
release and sale, its distribution is unlimited.

48

THE CAVITY AFTER VERTICAL WATER ENTRY

Prepared by:  
Albert May

ABSTRACT: At vertical water entry of a missile the splash varies greatly with nose shape and thus modifies the cavity development. Accordingly, the relations reported earlier, between cavities formed by different noses at oblique entry, cannot be applied to vertical entry.

An "Ideal Cavity" is defined as that portion of the cavity near the generating nose, which has not been appreciably affected by such influences as gravity or the difference between ambient pressure and the pressure in the cavity. It is shown that all such cavity portions are geometrically similar, with a size proportional to the square root of the drag force,  $(C_D A)^{1/2}$ , at a given speed.

PUBLISHED 12 JULY 1968

U. S. NAVAL ORDNANCE LABORATORY  
WHITE OAK, MARYLAND

NOLTR 68-114

12 July 1968

THE CAVITY AFTER VERTICAL WATER ENTRY

The author wishes especially to express his indebtedness to Mr. Jacob Berezow who reduced most of the research data, and to Mr. John L. Baldwin who supervised some of the water-entry tests.

E. F. SCHREITER  
Captain, USN  
Commander

*A. E. Seigel*  
A. E. SEIGEL  
By direction

# NOLTR 68-114

## CONTENTS

	Page
CHAPTER I, INTRODUCTION. . . . .	1
Cavity Comparisons and Correlation Techniques. . . . .	1
Cavity Events. . . . .	3
CHAPTER II, EXPERIMENTS. . . . .	5
CHAPTER III, CAVITY BEHAVIOR. . . . .	7
Pullaway . . . . .	7
Splash . . . . .	8
Deep Closure . . . . .	10
CHAPTER IV, THE "IDEAL CAVITY" . . . . .	12
CHAPTER V, CAVITY DEVELOPMENT. . . . .	20
Cavity Geometry. . . . .	20
Motion of the Cavity Wall. . . . .	21
REFERENCES . . . . .	22

## ILLUSTRATION

Figure	Title
1	Cavity Development After the Vertical Water Entry of a Sphere
2	Typical Deep Closure After Vertical Water Entry
3	Time of Pullaway After Vertical Water Entry
4	Splash Configuration Following the Vertical Water Impact of a Right Cylinder
5	Observed Flow in Water After Vertical Entry of a Sphere
6	Hydraulic Flow Model
7	"Ideal Cavity" from Parabolic Formula
8	Theoretical Cavity in Two Dimensions with Zero Cavitation Number
9	Ideal Cavity Due to a 1-1/2-Inch Sphere After Vertical Water Entry at 41 Feet per Second
10	Ideal Cavity Due to a 1/2-Inch Sphere
11	Ideal Cavity Due to a 1/4-Inch Right Cylinder
12	Ideal Cavity Due to a 45-Degree Cone
13	Ideal Cavity Due to the Vertical Water Entry of a 1-1/2-Inch Sphere at 116 Feet per Second
14	Length of Ideal Cavities for Right Cylinders
15	Calculated Ideal Cavities for a Right Cylinder and a 36-Degree Cone
16	Cavity Volume with and without Surface Closure
17	Development of the Cavity Due to Water Entry of a Sphere
18	Development of the Cavity Due to Water Entry of a Sphere
19	Development of the Cavity Due to Water Entry of a Right Cylinder
20	Change of Cavity Diameter with and without Surface Closure

## TABLES

Table	Title	Page
1	Characteristics of Models which Gave Data Used in this Report. . . . .	6
2	Distance Between Vertices of Analytic and Experimental Cavity Outlines . . . . .	19

SYMBOLS

a, b, c	Constants
A	maximum cross-sectional area of missile
$C_D$	drag coefficient
d	reference length: actual or equivalent diameter of nose flat, or D
D	maximum diameter of missile
f(r)	a function defining cavity growth
F	Froude number $\equiv v_o/\sqrt{gd}$ (usually $v_o/\sqrt{gD}$ )
g	acceleration of gravity
h	hydrostatic head
L	width of generating strip in equation 3
m	mass of missile
M	effective mass $\equiv m/\rho d^3$
n	trial exponent in outline equation
r	cavity radius at a given depth
s	distance along path of missile
S	$\equiv s/d$ , dimensionless distance ( $\equiv s/D$ in this report)
t	time measured from water impact (also a parameter in equation 3)
T	$\equiv tv_o/d$ , dimensionless time ( $tv_o/D$ in this report)
$T_{pa} \equiv \frac{t_{pa} v_o}{d}$	dimensionless time of pullaway ( $t_{pa} v_o/D$ in this report)
v	missile speed
$v_o$	missile speed at water impact
$v_1$	outward speed of cavity wall when its radius has some specific small value (say, unity)

$V$   $\equiv v/v_0$ , dimensionless speed  
 $x, y$  coordinates of cavity  
 $\rho$  mass density of fluid

## CHAPTER I

## INTRODUCTION

The air-filled cavity which follows a missile as it enters water from air has been the subject of numerous investigations (refs. 1, 2, 3, and 4), but only recently has an attempt been made (ref. 2) to correlate systematically the cavity development and collapse with experimental parameters. The principal purpose of the program described in the present report was to study the growth and collapse of cavities accompanying vertical water entry. A particular aim was to determine whether the violent collapse, which had been found to accompany "line closures" (ref. 2), occur after vertical water entry.

The growth and decay of the water-entry cavity have been described in detail (e.g., ref. 1) but a brief outline of the behavior will be given here. The nose of the missile gives a velocity (principally transverse) to the water, thus generating a cavity, and air rushes in from above the water surface to fill it. Later the splash converges just above the water surface and closes the cavity while it is growing. The resulting pressure reduction in the cavity causes it to move down from the water surface ("pullaway"). Still later the reduced cavity pressure and the ambient pressure due to depth cause the cavity walls to be pushed together, and a "deep closure" or seal, occurs. Usually, a series of deep closures occur and these cause a gradual (or sometimes rapid) decrease in the volume of the cavity attached to the missile.

#### Cavity Comparisons and Correlation Techniques

Certain dimensionless quantities which were defined in reference 2 will now be described. These quantities were originated in an attempt to systematize the development of the water-entry cavity by relating it to a small number of experimental parameters.

When the missile which is entering water is a right cylinder or has a nose which is well truncated, the water separates from the nose of the missile at the edge of the truncation. Accordingly, the nose-flat diameter is the only length that can be regarded as characteristic of the entry, and a Froude number may be defined as

$$F = v_0 / \sqrt{gd} ;$$

where  $v_0$  is the water-impact speed,  $g$  is the acceleration of gravity, and the reference length  $d$  is taken as the diameter of the nose flat. In reference 2, the mass of the missile was included in a quantity which was called the Effective Mass,

$$M = m/\rho d^3,$$

where  $m$  is the mass of the missile and  $\rho$  is the mass density of the water.

Missile speed, time, and path length can be nondimensionalized by writing:

$$v = v/v_0; \quad T = tv_0/d; \quad S = s/d.$$

A reference length (the missile diameter in this report) is taken as the unit length; unit time is the time ( $d/v_0$ ) required for the missile to travel a distance equal to the reference length at the entry speed; and unit speed is the speed at entry. Time is measured from the instant when the missile first touches the water.

It was further assumed in reference 2 that missiles whose noses are not truncated, such as hemispheres or ogives, generate cavities which are identical, for oblique entry, with those generated by right cylinders (or truncations) which experience the same drag force at the same speed. Based on this, an "equivalent nose-flat diameter" can be defined for the nontruncated nose, calculated from the drag. For example, if a sphere and right cylinder, when cavity-running, have  $C_D$  values of 0.3 and 0.8, respectively, the "equivalent nose-flat diameter" for a sphere will be  $\sqrt[3]{3/8} D = 0.612 D$ , where  $D$  is the sphere diameter.

This equivalence between noses with and without sharp truncations is based on an experimental result of reference 1; namely, cavities resulting from vertical water entry at a given speed are of almost identical shape if there is no surface closure and if the missiles have the same value of  $AC_D/m$ , i.e., if they have the same deceleration at the same speed. Under these conditions two missiles do work on the water at the same rate, and the flow caused by the missiles is nearly the same.

The pressure in the cavity usually decreases following a surface closure, and this can have a large effect on cavity development and cavity shape. For the entries of reference 2, because of the obliquity, the cavities became large before surface closure, and the ensuing pressure changes were small. It will be shown later that equivalence (with equal drag forces) was not found between right cylinders and spheres in the present program. This is because surface closure occurs earlier for vertical entry, and quite differently for the two shapes.

This scaling failure raised the question as to whether  $M$  and  $F$  (based on equivalent nose-flat diameter) are still suitable parameters for the presentation and comparison of data for vertical entry. It appears that they are suitable parameters if only hydrodynamic and hydrostatic forces are significant, but not if the pressure in the cavity differs considerably from the pressure above the water and if the difference has a significant effect on the behavior.

On the other hand, in comparing such noses as spheres and right cylinders at vertical entry, a quantity like cavity-volume-after-surface-closure depends on the nose shape in a manner unrelated to the drag force alone, and no parameter is known which would furnish a basis for comparison. Unless such a parameter is found, the two sets of data cannot be compared as parts of a combined set.

In the present report, model diameter,  $D$ , has been used as the characteristic length in forming dimensionless quantities, except in the case of  $M$ . The quantity  $M$  is principally significant in its relation to acceleration, and for acceleration nose-flat diameter, real or equivalent, is most important.

### Cavity Events

Figure 1 (which is copied from reference 1) includes four frames from the high-speed motion picture of a cavity following the typical vertical water entry of a sphere. The first frame shows the initial above-water splash. In the second frame the splash is doming over to form surface closure. In this frame the closure is probably not quite complete, but this cannot be appraised by eye. The jet, which is traveling downward, is merely spray entrained in the air flowing into the cavity. Unfortunately, surface closure is not useful in comparing cavities because the completion of closure cannot be observed.

The third frame was taken just after pullaway. The black area between the top of the cavity and the water surface is a cloud of small bubbles. At this point the downward jet has become a "solid" jet rather than spray. Usually its speed, relative to the top of the cavity, is quite slow. Pullaway of the cavity from the water surface is the most useful event in comparing cavities because it can be determined with good accuracy.

The last frame shows deep closure. The time and position of some types of deep closure can be determined accurately, but the deep closures, which follow vertical entry from air at ordinary atmospheric pressure, are generally difficult to appraise. It is impossible to say exactly when the closure is complete. The well-contoured top of the lower cavity in the photograph suggests that deep closure was complete slightly before the photograph was taken. One is tempted to measure the volume of the detached upper cavity segment from the geometry apparent in the photograph. This may be a very bad approximation as can be seen from the photograph

in figure 2. The cavity narrows at a point rather near its upper end, and at the same time a jet travels downward from the top. Sometimes the upper end of the cavity is a uniform cylinder which becomes filled by the jet, so that the upper cavity portion simply disappears, with the earlier position marked only by a few small bubbles. More frequently (as in fig. 2) the jet entirely fills the neck but not the segment above it. The result is that a little later a few bubbles of rather small size emerge from a bubble cloud in which the individual bubbles cannot be resolved and their contribution to the volume cannot be estimated.

## CHAPTER II

### EXPERIMENTS

The vertical water-entry data analyzed in the present report came from two groups of experimental work: tests made for the purpose in the Pilot Hydroballistics Facility at the Naval Ordnance Laboratory (ref. 5), using cylinders with flat, hemisphere, and cone noses; and tests, principally with spheres, made some years ago (ref. 1). Table 1 lists the characteristics of the later models which provided data used in the present report.

Initially models with flat noses were constructed with values of  $M$  approximately equal to 9, 18, 50, and 100. All were simple steel right cylinders. Models with  $M = 18$  were designed for tests to be compared with those of steel spheres. All steel spheres have  $M = 17.7$  and much sphere data were available. Models with  $M = 100$  were designed as most suited to produce line deep-closures, which collapse with greatest violence.

The new large Hydroballistics Tank at NOL was not completed in time for this research, and a limited program was carried out in the small Pilot Tank principally with the lighter models ( $M = 9$  and 18).

TABLE 1  
CHARACTERISTICS OF MODELS WHICH GAVE DATA USED IN THIS REPORT

Nose shape	Diameter inches	Weight pounds	Length inches	M	Material
right cylinder	1/2	0.077	1.47	17.1	steel
	1	0.65	2.93	19.9	"
	1	1.84	8.26	50.9	"
	1-1/2	1.07	2.09	8.8	"
	1-1/2	2.14	2.00	17.6	tungsten
	1-1/2	2.19	4.38	17.9	steel
	1-1/2	6.19	12.40	50.7	"
	1-1/2	0.45	1.30	17.7	"
sphere	1-1/2	0.43	4.50	15.4	aluminum
hemisphere	1-1/2	2.33	5.75	97.6	steel
45° cone	1-1/2	2.16	4.75	34.7	"
90° cone	1-1/2				

### CHAPTER III

#### CAVITY BEHAVIOR

##### Pullaway

Pullaway, or the motion of the upper end of the cavity down from the water surface, is brought about as follows. When surface closure seals the upper end of the cavity, the cavity becomes a closed envelope containing an almost fixed quantity of air. At the time of surface closure the cavity is usually increasing in size. As the cavity grows adiabatically the pressure of the contained gas drops. As the pressure goes below atmospheric the higher (atmospheric) pressure above the water surface, and above the cavity, causes the cavity to move downward. Water flows in from around the cavity to prevent the creation of a void above the cavity due to its descent. As this converging flow meets in the center above the cavity, its energy goes into the creation of jets; upward and downward to satisfy the momentum condition.

The amount of pressure drop in the cavity, due to its expansion, determines the speed with which the cavity travels away from the water surface. At very low entry speeds the cavity pressure does not drop appreciably and the cavity moves downward very slowly or even remains attached to the water surface. While pullaway is caused entirely by the pressure drop in the cavity, deep closures, if they represent lateral collapses of the cavity, are due to the pressure differential between the cavity and its surroundings, including both the decrease of cavity pressure and the increase of ambient pressure due to depth of immersion.

There are several reasons why pullaway is especially useful in comparing water entries; it almost always occurs, it is easily photographed, and the instant of separation can be determined with good accuracy. This is true for both vertical and oblique water entry.

Figure 3 contains plots for a number of model designs, of the dimensionless time of pullaway against Froude number based on missile diameter, after vertical water entry. The graphs are least-square straight lines calculated for each of the missile designs. A few (unshown) data points were dropped from the calculation because of apparent inaccuracy.

In particular, data for low-speed spheres were not included for the following reason. Data were available (from the study of reference 1) for steel spheres with diameters between 1/4 and

1-1/2 inches. The scaling of the dimensionless time of pullaway was found to be very poor, in the comparison of the small and larger spheres, with much lower times for the small spheres. Study showed that the nonconforming small spheres had Reynolds numbers (based on impact speed and the length of flow on the sphere) below about  $3 \times 10^5$ . Above this Reynolds number the agreement was good. It appears probable that the point where the flow separates from the sphere changes at a critical Reynolds number.

While the time of pullaway varies greatly with missile design, the slopes of the graphs in figure 3 are very nearly the same. This figure shows that the dimensionless time of pullaway,  $T_{pa}$ , always increases as  $F$  increases. The actual time,  $t_{pa}$ , on the other hand, decreases as  $F$  increases but not fast enough to make  $tv_0$  decrease. For oblique entry at higher speeds, reference 2 showed that the actual time of pullaway increases as the speed becomes greater. This doubtless results from the decreased rate of mass flow into the cavity at high speeds.

The three lowest graphs of figure 3 are for right cylinders with three values of the Effective Mass,  $M$ . The variation of  $T_{pa}$  with change of  $M$  is easily explained. The lighter cylinders (lower value of  $M$ ) decelerate more than the heavier ones. Hence, their cavities are smaller, the speed of the intruding air is less, and the pressure in the cavities is greater. The higher pressure in the cavities for the lighter cylinders delays the time of pullaway.

The variation of  $T_{pa}$  with nose shape (flats, spheres, or cones) is undoubtedly due to the splash, which will be discussed in the next section. The fact that graphs for spheres and cylinders having the same value of  $M$  ( $M = 18$ ) are nearly parallel, means that the spheres are deeper than the cylinders by an almost constant distance (6 or 7 diameters) when pullaway occurs.

If Froude number, in figure 3, had been related to equivalent nose-flat diameter rather than to missile diameter, the separation of the graphs for different nose shapes would have been still greater. If the difference in pullaway time is due to the configuration of the splash, it is improbable that any choice of characteristic length would have significance.

All missiles which contributed data for figure 3 had the same diameter (1-1/2 inch). Hence, at the same Froude number, the ratio of actual times equals the ratio of dimensionless times.

### Splash

The different time of pullaway observed for noses of different shapes (e.g., spheres and flats) is rather evidently due to a

different splash configuration. The time of pullaway depends strongly on the time of surface closure since closure is followed by a reduction of cavity pressure. The time of surface closure is greatly influenced by the nose shape through its effect on the splash pattern.

In the first two photographs of figure 1, the above-water splash and the cavity wall are seen on either side of the meniscus at the water surface. It is important to distinguish the splash from the cavity wall. Splash generation occurs only during the impact and flow-forming phases of water entry and is not a continuing process. After the nose is well below the water surface the water particles that receive energy from the missile do not detach from the liquid mass. The lower end of the splash sheath remains attached to the meniscus at the water surface and this is at the lip of the cavity. Before surface closure there is no appreciable flow up or down the cavity wall. Hence, after the nose is wetted there is probably no addition of water to the splash. The splash sheath becomes taller and broader following generation, so, presumably, it becomes thinner, and maintains its integrity because of surface tension.

It is the relation of splash to flow formation which causes its great dependence on nose shape. Splash due to a sphere is formed by the flow which escapes the high-pressure region by moving tangent to the sphere's surface. The angle changes as penetration progresses. The most evident splash (that which causes surface closure) travels initially at an angle of about 60 degrees to the water surface. An earlier splash is often apparent, traveling at a much lower angle.

For the flat nose, horizontal escape of the accelerated water is difficult and the pressure is relieved by a flow at an angle of about 75 degrees from the horizontal. The cavity outline and splash are sketched in figure 4 for six instants after vertical water entry of a tungsten right cylinder. The ticks external to the outlines denote the height of the undisturbed water surface.

The cavity wall appears to be almost in contact with the cylindrical wall of the missile in the early phases of its growth. The seal cannot be airtight, however, because of the rapid increase of the cavity volume. Nevertheless, surface closure and pullaway are much more rapid for the flat than for the sphere. A small angle of attack of the right cylinder causes great asymmetry of the splash.

A little study of the splash outlines of figure 4 shows that a very different behavior may be expected if the nose of the missile, instead of being flat, is an ogive or cone, truncated to less than half the missile diameter. The splash must then strike the surface of the nose, and the cavity may close rapidly and its growth be greatly reduced. This should be investigated experimentally. (The missile's nose may contact the splash but remain far from the cavity wall.)

For 45- and 90-degree cones the splash seems to have an initial direction approximately bisecting the angle between the cone surface and the water surface. After the flow is established, the water moves parallel to the conical surface.

It should be noted that the strong effect of nose shape on splash, surface closure, and pullaway has been demonstrated here only for vertical water entry. The effect was not observed in the analysis of the oblique entries of reference 2. It appears that there is much less effect on nose shape as the entry goes away from the vertical. Whether or not the splash differs greatly, the effect on later behavior is less because surface closure is delayed by the larger opening which must be closed at the water surface.

### Deep Closure

In reference 2, three types of deep closure were described and were given the names "point closure," "base closure," and "line closure." In line closures a length of cavity collapses onto its axis almost simultaneously. Line closures were believed to be especially violent since considerable breakage of underwater lights accompanied them. A specific aim of the present program was to determine whether such closures could be observed after vertical entry, with a suitable choice of experimental parameters.

Reference 2 indicated that the oblique entry of a missile may cause a line closure if  $M \geq 25$ , only slightly higher than the value of  $M$  for a steel sphere ( $M = 18$ ). The minimum value of  $F$  for which line closures were obtained, however, was about 300. This corresponds to an entry speed of 345 feet per second for a 1/2-inch right cylinder, and higher speeds for larger missiles. Unfortunately, during the present program, limitations on size, weight, and speed did not permit duplication of the conditions found suitable for the production of line closures during oblique entry. Few entries with missiles having  $M > 18$  behaved satisfactorily.

No line closures were observed, nor was there indication of an approach to this condition. From the experimental evidence one cannot determine whether heavier models might produce line closures after vertical entry.

For the vertical entry of lightweight models, little variation was observed in the appearance of the cavity at deep closure. The portion of the cavity which detaches from the missile is always small. The deep closure following the entry of spheres looks like a point closure (see ref. 1 and fig. 2) but the detached portion of the cavity proves later to contain only small bubbles as already mentioned. The size of the detached bubble increases slightly as the entry speed increases. The cavities produced by right cylinders have base closures which leave behind trails of small unresolved bubbles.

NOLTR CG-114

Usually a succession of deep closures occurs after vertical entry. Between the closures, re-entrant jets are frequently evident, and these sometimes cause deformation of the cavity.

# CHAPTER IV

## THE "IDEAL CAVITY"

As a missile travels through water it loses some of its energy to the water, through the drag force. Presumably the velocity given to the water is proportional to the square root of the drag coefficient and to the speed of the missile. It has been observed after vertical entry (ref. 1), that imperfections on the cavity wall have little longitudinal motion as the cavity enlarges, that is, the motion on the cavity wall is almost perpendicular to the trajectory, and horizontal for vertical entry. (After pullaway there is a considerable flow on the upper cavity wall. Presumably, at that time, the flow up the cavity wall feeds the jet which passes downward into the cavity.)

For simplicity it might be assumed that the energy given to the water while the missile travels unit distance is stored in a horizontal lamina of unit thickness, were it not for two difficulties: an infinite plane lamina would have infinite energy; and the flow is observed to curve upward later toward the water surface (ref. 6). This is shown by the flow lines in figure 5 which is reproduced from reference 7. The upward flow lines observed by Birkhoff led him to propose a model in which the flow is within spherical shells centered at the water-entry point (fig. 6). Let us assume that the energy is stored conservatively in either a lamina or a spherical shell, with or without gravity forces. As the cavity section (the inner void in the shell) expands, the speed of the flow decreases because of forces arising from the continuity conditions. Roughly, the speed of the wall, during the cavity expansion, will be inversely proportional to the cavity diameter.

No one could study large numbers of cavities generated by missiles, without observing the great similarity of the portion of the cavities nearest the generating nose of any particular missile. The similarity is found over a wide range of speeds and depths. Based on this observation we shall define an "ideal cavity" and consider its generation by a missile traveling into or through the water.

Any cross section of an "ideal cavity" would be generated under the following conditions and assumptions:

1. The speed of the missile is constant;
2. Gravity is absent;

3. The pressure in the cavity is the same as in the water surrounding it;

4. In the absence of forces due to gravity and pressure, it is assumed that the growth history of any cavity section depends only on the speed initially given to the cavity wall and the cavity diameter when it had this speed. In particular, it is assumed that the section develops at the same rate whether the cavity is being generated very near the water surface or at a considerable depth in the water. (In this chapter, "ideal" or "ideal cavity" will be used only to designate the cavity as defined above.)

When the cavity pressure and ambient pressure are equal, the cavity should presumably be closely related to the infinite classical cavity of zero cavitation number. On the other hand, the ideal cavity as here defined is not the infinite, classical cavity, but any portion of it (near the vertex). This aspect of the ideal cavity will now be clarified by consideration of several assumed cavities.

Suppose that a moderately high-speed missile, 1 inch in diameter, has entered the water vertically and penetrated a distance of four inches, with the generation of a cavity. This cavity will approximate the "ideal cavity" because gravity has not had time to affect it appreciably nor has any slight pressure deficiency within the cavity. We assume then that it is (entirely) an ideal cavity. If the cavity outline is examined again after four inches more of water penetration, and if the 8-inch outline is compared with the 4-inch one first considered, it will probably be found that they superimpose almost exactly in their common (4-inch) section nearest the generating nose. (Evidently the upper 4-inch section of the longer cavity cannot be compared with the earlier cavity.) Hence, both of these 4-inch sections constitute ideal cavities. Whether the cavity is ideal also over the remaining 4-inch section depends on the basic condition, whether this portion has been deviated by other forces from its ideal shape. If it has not been, then we regard the whole eight inches of the cavity, or any part of it surrounding the vertex, as an ideal cavity.

After the missile has descended much further into the water and the cavity has closed above the water surface, it might be found that only about three inches of the cavity are identical with the corresponding section of the 4-inch cavity first considered. Then, in the longest cavity only the first three inches constitute an ideal cavity. However, this 3-inch portion is regarded as an ideal cavity even though the remainder of the cavity is not ideal. Various assumptions have been expressed or implied in this argument, and these will be justified in the following paragraphs.

The graph of figure 13 (on the transparent pullout sheet) is a cavity outline from the vertical water entry of a 1-1/2-inch sphere at 116 feet per second (P-322). The air pressure above the water had been reduced to 1/8th atmosphere to prevent surface-closure of the cavity. This cavity was chosen as being almost ideal. The

outline on figure 13 is actually drawn one-half true size. The unit used is the sphere diameter, D. It will be shown later that this half-scale drawing is actually the outline of the ideal cavity which would be generated by a 3/4-inch sphere, and an equation will now be derived for the graph of figure 13.

First, the equation was assumed to be of the form

$$x + a = by^n \quad (y > 0)$$

Values of y corresponding to integral values of x were read from the graph of figure 13. A least-square determination was made of the values of a and b for an assumed value of the exponent n. This was repeated for other values of n to determine the n value giving the best least-square fit. The best fit was obtained for  $n = 2.0$  and

$$x + 0.438 = 3.133y^2 \quad (1)$$

where the unit is the sphere diameter.

Equation (1) is plotted on figure 7. If the transparent sheet containing figure 13 is pulled out, its graph can be superposed on the graph of figure 7, so that the agreement of the curves can be observed. Figure 13 is bound in this report at such a position that it can be compared similarly with the graphs of figures 8, 9, 10, 11, and 12. The axial line and the cross on the axis of the graph of figure 13 are to be superimposed on the axis and cross on each of the comparison figures, for best agreement of the curves.

The comparison of figures 13 and 7 shows that the parabola of equation (1) fits the data rather well. The average difference of the analytic and experimental curves is 1.8 percent up to  $x = 6D$  or 4.2 percent up to  $x = 9D$ . Actual cavities usually have a considerable section which is nearer to being conical than is the analytical outline of equation (1).

It is not expected that the empirical curve of figure 13 is a highly accurate trace of the ideal cavity. Some hydrostatic head was present during this cavity development and the sphere decelerated slightly.

Mention has been made of the classical cavity of zero cavitation number. The equation of the outline of this cavity has never been determined theoretically for the three-dimensional case. Levinson (ref. 8) found a formula for the asymptotic shape of this cavity:

$$y = \frac{cx^{1/2}}{(\log x)^{1/4}} \left( 1 - \frac{1}{8} \frac{\log \log x}{\log x} + \dots \right) \quad (2)$$

This equation is valid only far from the missile nose, and the ideal cavity is valid only near the nose. The functional agreement between the two is reasonable.

An exact solution is given in reference 9 for the two-dimensional analog of the ideal cavity, the two-dimensional cavity with zero cavitation number. It is written in the parametric form

$$\left. \begin{aligned} x &= \frac{L}{4 + \pi} \left[ t \sqrt{t^2 - 1} - \log(t + \sqrt{t^2 - 1}) \right] \\ y &= \pm \frac{L}{2} \pm \frac{2L}{4 + \pi} (t - 1) \end{aligned} \right\} \quad (3) \quad t = 1$$

Here,  $L$  is the width of the infinite strip that threw the cavity, and  $t$  is merely a connecting parameter. Equation (3) was compared with figure 13 to see how similar the two- and three-dimensional outlines might be. Figure 8 is a plot of equation (3) with  $\tau = 0.760$ , a value which gives the best agreement with figure 13. The agreement is excellent.\*

Certain assumptions as to the generation and growth of cavities will now be stated. Although these may appear to be gross simplifications, examination will show that they give approximations which are quite good within properly restricted limits. These assumptions are:

a. The velocity,  $v_1$ , given to the cavity wall by the missile is proportional to  $(AC_D)^{1/2}$ . The velocity  $v_1$  is the velocity at some arbitrary small cavity radius. The assumption is made here that the velocity given to the water depends on the missile speed only through the total drag force.

b. The speed of the cavity wall at any radius  $r$  is  $v_1(r)$ , where  $f(r)$  is a unique function of the cavity radius only, dependent on the continuity equation.

c. The time required, at any depth, for the cavity to expand between any two radii is inversely proportional to  $v_1$  (at a given radius).

\*This leads to the interesting observation that the rather complicated equation (3) can be approximated by a parabola. Specifically, the equation

$$x/L + 1.00 = 1.598(y/L)^2$$

gives the same value as equation (3) to within 1.0 percent for  $1.7 < x < 23$  and within 2.4 percent for  $1.3 < x < 55$ .

Under the assumptions above, all ideal cavities should be geometrically similar. This will be demonstrated by the arguments which follow, and will be verified by experimental data.

a. Two scaled models of different size will generate ideal cavities which are geometrically similar and proportional to the model size. This is almost axiomatic. It is a special case of item d below.

b. The shape of the ideal cavity due to a particular missile is independent of its speed. For, if the speed is doubled, the time to travel a given distance is halved and so is the time to reach a given cavity radius at any cavity cross section. Hence, during a particular water entry the shapes of all ideal cavities are identical.

c. Two missiles, whose drag forces are the same, generate identical cavities which are identical except immediately behind the generating noses. Such missiles might be a one-inch right cylinder ( $C_D = 0.8$ ) and a 2-inch 36-degree cone cylinder ( $C_D = 0.2$ ).

An experimental demonstration of this for vertical entry was described in reference 1.

d. Ideal cavities formed by the water entry of missiles having different drag forces at the same speed will be geometrically similar, with dimensions proportional to  $(AC_D)^{1/2}$ .

On the basis of these statements, equation (1) for the ideal-cavity outline can be modified to the form

$$\frac{x}{nC_D^{1/2}} + a = b \left( \frac{y}{DC_D^{1/2}} \right)^2.$$

The equation finally takes the universal form

$$\frac{x}{DC_D^{1/2}} = 1.716 \left( \frac{y}{DC_D^{1/2}} \right)^2. \quad (4)$$

In equation (4) the curve has been displaced so that its vertex is at the origin of coordinates. The distances between the vertices of the analytical and experimental outlines will be discussed later.

In summary, it is claimed that ideal cavities are

a. identical when formed by the same missile at different speeds,

b. proportional to the missile size when formed by two missiles identical except for size, and

c. proportional to the square root of the drag forces at the same speed, when formed by dissimilar missiles.

Comparisons of pairs of cavities in each of these situations can be made between figures 9, 10, 11, or 12, and the pullout, figure 13. Figure 9 gives the half-scale cavity outline for a 1-1/2-inch steel sphere entering water vertically at 41 feet per second. The agreement with the outline of the pullout sheet, figure 13, is almost exact, although the speeds of the two spheres were 41 and 116 feet per second.

Figure 10 gives a half-size cavity trace for a 1/2-inch steel sphere entering at 208 feet per second, and the same outline magnified by a factor of 3. The agreement between the enlarged outline and that of a 1-1/2-inch sphere on figure 13, is reasonably good, showing that cavity sizes are proportional to missile sizes.

The small outline on figure 11 is that of a cavity due to a 1/4-inch right cylinder entering water at 37 feet per second. For comparison with the cavity of a 1-1/2-inch sphere we multiply by

$$\frac{D_1 C_{D_1}^{1/2}}{D_2 C_{D_2}^{1/2}} = \frac{1.5 (0.3)^{1/2}}{0.25 (0.8)^{1/2}} = 3.68. \quad \text{For the comparison with the half-}$$

size outline of figure 13, we use a factor half as great, or 1.84. This factor gave the larger outline of figure 11. The agreement with figure 13 is very good except near the generating nose where the cavities cannot be expected to agree.

Figure 12 gives the outline of the cavity due to a 1-1/2-inch 45-degree cone cylinder which entered the water vertically at 139 feet per second. For comparison with figure 13 the magnification was calculated, as before, from the formula

$$\frac{1}{2} \frac{D_1 C_{D_1}^{1/2}}{D_2 C_{D_2}^{1/2}} = \frac{1}{2} \frac{1.5 (0.30)^{1/2}}{1.5 (0.27)^{1/2}} = 0.527$$

and the outline on figure 12 was made using this reduction factor. The agreement of figures 12 and 13 is very satisfactory.

The good agreement which has been apparent in each case is typical. In general, only early cavities are ideal and comparable, that is, only portions which have not existed very long. All cavities of sufficient length will fail to agree or, more precisely, some forward portion of such cavities will be ideal but the aft

end will not. The extent of this agreement is shown in figure 14, where the length of the cavity portion which is ideal is plotted for 1/4-inch and 1/2-inch right cylinders, with air pressures above the water of 1/2 atmosphere or less. The data on figure 14 were obtained by comparing cavity outlines produced by the entry of such cylinders at various speeds, with outlines sketched from equation (4). The ordinate in figure 14 is the axial length of the cavity whose diameter agreed with equation (4) to within 10 percent. The graphs drawn are a least-square family of parallel straight lines, one for each air pressure. The spacing of the lines was probably affected by the distribution of data between the two missile sizes. The length of the ideal portion of the cavity increases as the pressure of the atmosphere above the water decreases because surface closure and the resulting cavity-pressure reduction are delayed.

The fact that all ideal cavities are geometrically similar appears at first to be inconsistent with the easily observed fact that the cavities thrown by blunt bodies are broad and those due to fine bodies are narrow. That these cavities may still be similar can be seen from a study of figure 15. Curve A was calculated from equation (4) for a right cylinder ( $C_D = 0.8$ ) and curve B for a 36-degree cone cylinder ( $C_D = 0.2$ ) of the same diameter. Evidently from equation (4) these curves are geometrically similar. When curve B is transformed into curve A by multiplying both coordinates by 2, only the solid line portion of curve B contributes to the plotted portion of curve A.

It is interesting that B can also be transformed into A merely by dividing its axial length-coordinates by 2. It is evident, of course, that the same result cannot be obtained by doubling the radii of B. This would require that the radial speed were constant and not a function of  $r$ .

One difficulty in comparing ideal cavities is that the vertices of the analytical and experimental cavities cannot be expected to coincide. The definition of the ideal cavity leads to its shape but not to the position of its vertex relative to the missile. In particular, the formula does not represent the cavity immediately behind the missile nose and equation (4) gives a cavity whose vertex is usually in front of the missile. It is important to know this separation since applications of the ideal cavity concept usually involve the position of the missile relative to the cavity walls.

Comparisons of the computed cavity shapes with photos yielded the approximate distances of the computed vertex in front of the forward tip of the nose given in Table 2.

From the discussion of the present chapter it is evident that the concept of the ideal cavity is in reasonable agreement with observed cavity shapes. When cavities deviate from the ideal shape, the usual cause is either a reduced pressure in the cavity or hydrostatic head,

TABLE 2

DISTANCE BETWEEN VERTICES OF ANALYTIC AND  
EXPERIMENTAL CAVITY OUTLINES

(A positive value indicates that the vertex of the computed outline is ahead of the nose tip of the missile.)

<u>Nose Shape</u>	<u>Distance between vertices (in calibers)</u>
Sphere	0.5
Right cylinder	0.4
45-degree cone	-0.2

and these will cause parts of the cavity to be narrower than the ideal cavity. Hence, the ideal cavity may be taken as a limiting size of the cavity close to the cavity-generating nose. If the missile's afterbody does not extend beyond the outline of the ideal cavity, it may be entirely within the actual cavity, if the cavity is ideal at the important cross section.

It should be noted that the examples which have been given, of cavities which are reasonably ideal, were all for entries with reduced air pressure above the water. With atmospheric pressure the portion of the cavity which is ideal is somewhat smaller.

## CHAPTER V

### CAVITY DEVELOPMENT

#### Cavity Geometry

Almost all water-entry cavities, created under natural atmospheric conditions, close above the water surface. The closure is slower for oblique than for vertical water entry and it can be delayed or prevented by reducing the pressure of the atmosphere above the water. Various artificial means have been used to accelerate, delay or prevent the closure. For example, a sphere dipped into a wetting agent, and then dropped into water without drying, was observed to produce a very large cavity, apparently because the splash sheath disintegrated. The maximum volume reached by a water-entry cavity depends strongly on whether, and when, a surface closure occurs.

In figure 16 cavity volume is plotted against dimensionless time for two vertical water entries of a 1-inch steel sphere at 96 feet per second. One of the entries (R-548) was from air at ordinary pressure but for the other (R-423) the pressure above the water was reduced to 1/29th atmosphere so that no surface closure occurred. The open cavity grew to a volume greater than  $500 D^3$ , but the closed cavity reached only  $43 D^3$ . This shows the great influence of surface closure on the maximum cavity volume. The increase of the volume of the open cavity was terminated by a deep closure which left only a volume of  $23 D^3$  attached to the sphere.

Figure 17 gives an enlarged curve of the cavity volume after the vertical entry of a 1-inch sphere at 96 feet per second, with atmospheric pressure above the water (R-548). Figure 18 contains a similar curve for a 1-1/2-inch sphere which entered vertically at 125 feet per second. The figures also contain graphs of cavity length and maximum diameter as functions of dimensionless time.

On figure 19 are given the volume, length, and diameter curves for the cavity due to a 1-1/2-inch right cylinder. The missile which generated this cavity had the same value of  $M$  as the steel spheres ( $M = 18$ ). The entry speed was 145 feet per second.

The time of pullaway is indicated on the volume curves. It is seen to occur very shortly before maximum volume for the sphere entries. For the entry of a right cylinder (fig. 19) maximum volume occurs long after pullaway and has a value twice the volume at pullaway. On all figures, cavity length is shown as increasing

up to the time of deep closure. Cavity diameter reaches a maximum and then decreases. Maximum cavity volume occurs just after the cavity diameter has passed its maximum.

#### Motion of the Cavity Wall

After vertical entry of a missile, the cavity wall at any depth travels outward horizontally until it reaches some maximum diameter and then collapses to zero or onto the air trapped in the cavity. The wall completes its outward and inward motions more rapidly when the volume is limited by a surface closure. A comparison is given in figure 20 of the expansion and contraction of open and closed cavities at a 7-inch depth. The rounds are the same 1-inch steel spheres whose volumes were plotted on figure 16. The wall of the open cavity took much longer to complete its outward travel and reached a diameter of 6.5 inches, while the closed cavity expanded only to 2 inches.

REFERENCES

1. May, A., "Vertical Entry of Missiles into Water," J. Appl. Phys. 23, 1362 (1952); also NAVORD Report 1809 (1951)
2. May, A., and Hoover, W. R., "A Study of the Water-Entry Cavity," NOLTR 63-264 (1963)
3. Waugh, J. G. and Stubstad, G. W., "Water-Entry Cavity Modeling, Part 1 - Vertical Cavities," NAVORD Report 5365, NOTS 1597 (1956)
4. Waugh, J. G. and Stubstad, G. W., "Water-Entry Cavity Modeling, Part 2 - Oblique Cavities," NAVORD Report 5365 NOTS 1890 (1957)
5. Seigel, A. E., "The Hydroballistics Facility at NOL," NOLTR 66-125 (1966)
6. Birkhoff, G. and Caywood, T. E., "Fluid Flow Patterns," NAVORD Report 447 (1947) or J. Appl. Phys. 20, 646 (1949)
7. Birkhoff, G. and Isaacs, R., "Transient Cavities in Air-Water Entry," NAVORD Report 1490 (1951)
8. Levinson, N., "On the Asymptotic Shape of the Cavity Behind an Axially Symmetric Nose Moving Through an Ideal Fluid," Ann. Math. 47, 704 (1946)
9. Gilbarg, D., "Jets and Cavities," Encyclopedia of Physics, Vol. IX, Fluid Dynamics III, Springer Verlag, Berlin, p. 329 (1960)

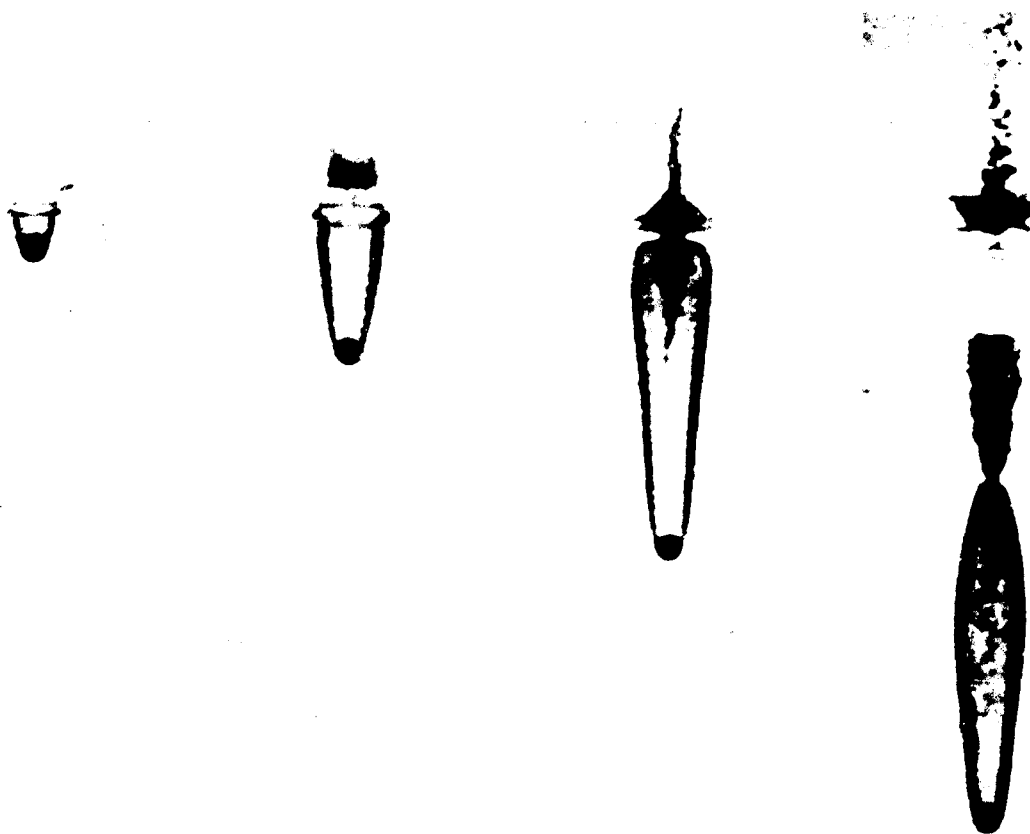


FIG. 1 CAVITY DEVELOPMENT AFTER THE VERTICAL WATER ENTRY OF A SPHERE

NOLTR 68-114

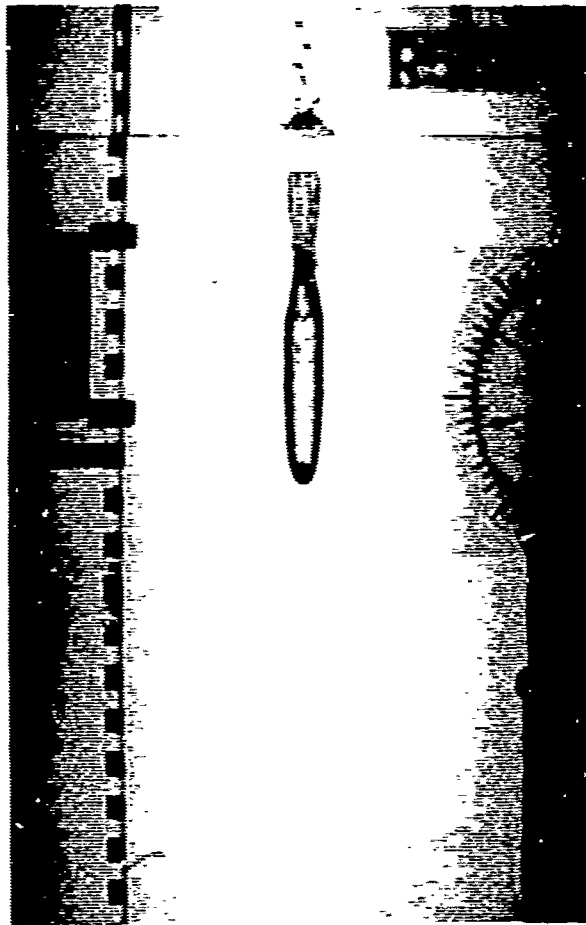


FIG.2 TYPICAL DEEP CLOSURE AFTER VERTICAL WATER ENTRY

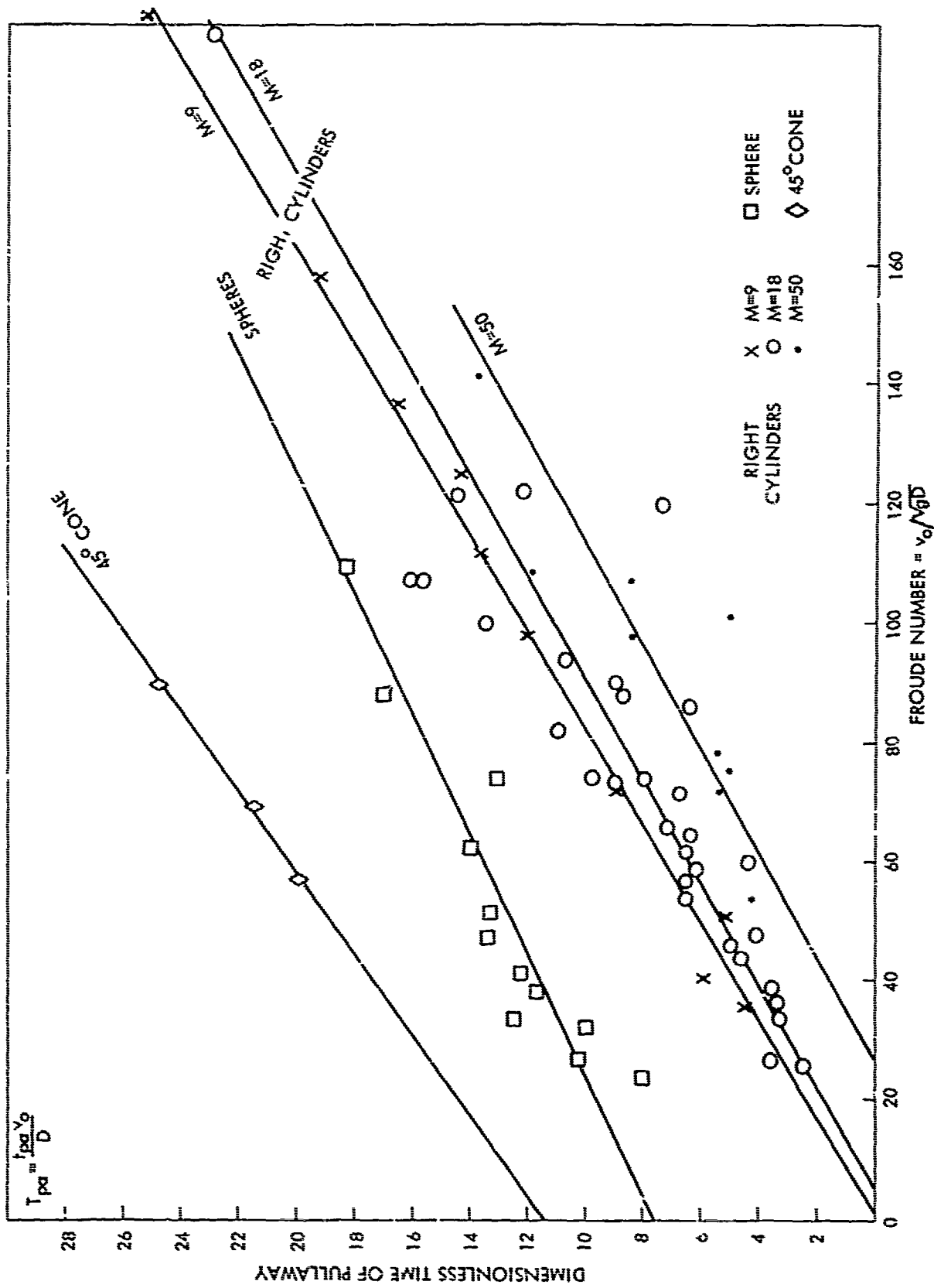


FIG.3 TIME OF PULLAWAY AFTER VERTICAL WATER ENTRY

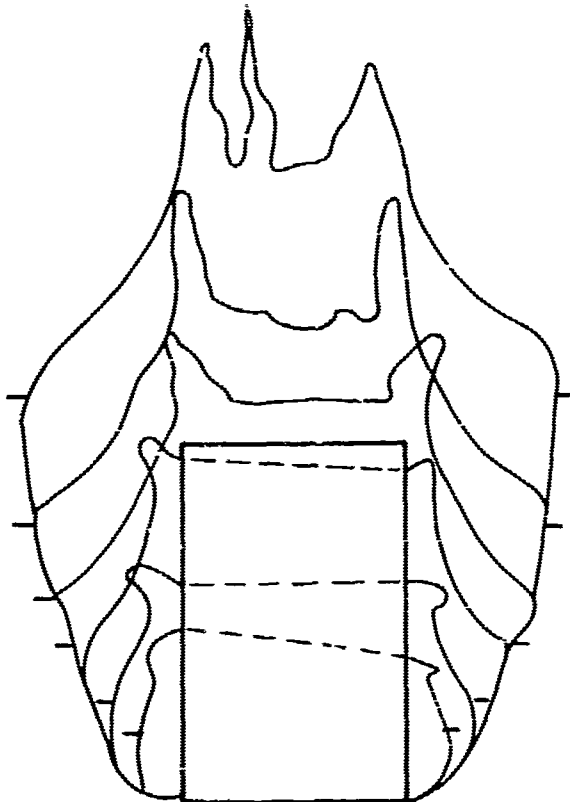


FIG.4 SPLASH CONFIGURATION FOLLOWING THE VERTICAL WATER IMPACT OF A RIGHT CYLINDER

TICKS INDICATE THE HEIGHT OF THE ORIGINAL WATER SURFACE FOR EACH SPLASH OUTLINE

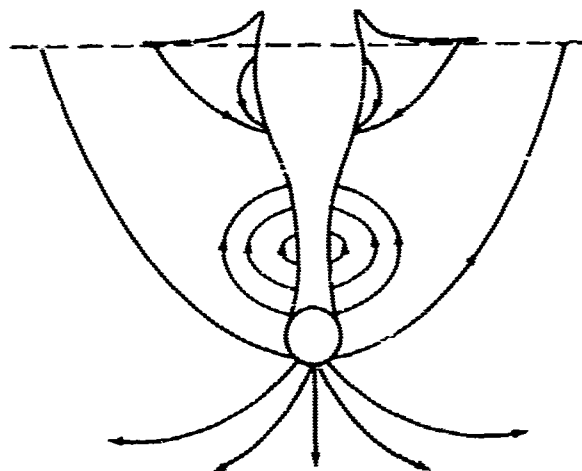


FIG.5 OBSERVED FLOW IN WATER AFTER VERTICAL ENTRY OF A SPHERE (AFTER BIRKHOFF AND ISAACS)

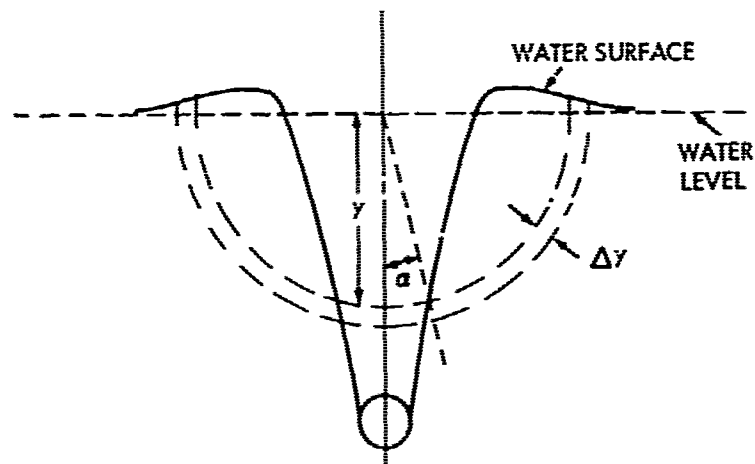


FIG.6 HYDRAULIC FLOW MODEL (BIRKHOFF AND ISAACS)

NOLTR 68-114

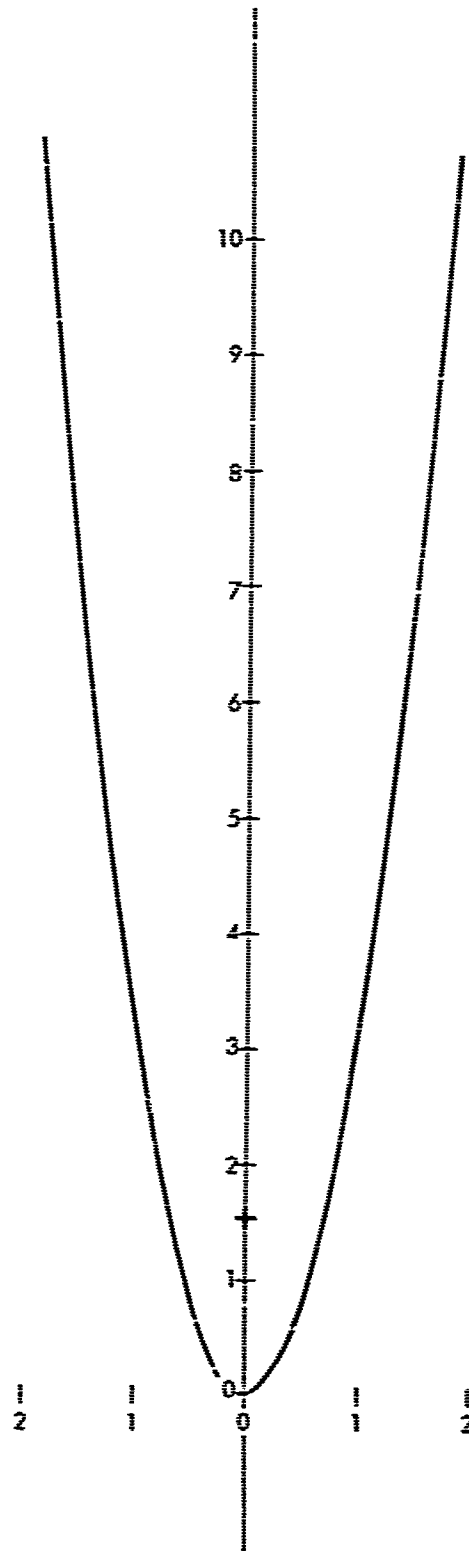


FIG.7 "IDEAL CAVITY" COMPUTED FROM PARABOLIC FORMULA FOR A 3/4-INCH SPHERE.  
COORDINATES ARE IN SPHERE DIAMETERS

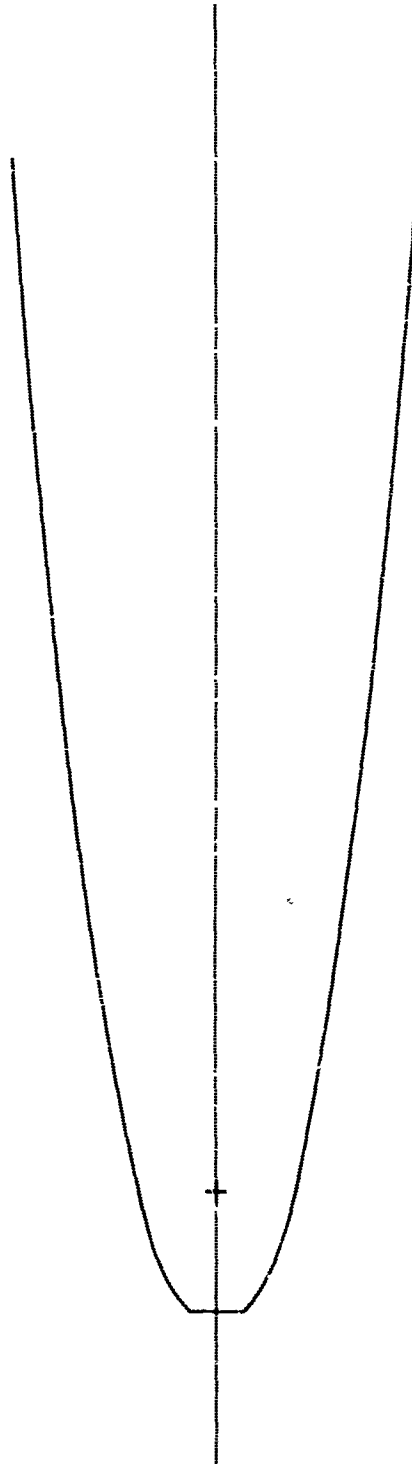


FIG.8 THEORETICAL CAVITY IN TWO DIMENSIONS WITH ZERO CAVITATION NUMBER,  
THROWN BY A NARROW STRIP  
AN OBSERVED IDEAL CAVITY (FIG. 13) CAN BE SUPERIMPOSED ON THIS  
OUTLINE, FOR COMPARISON

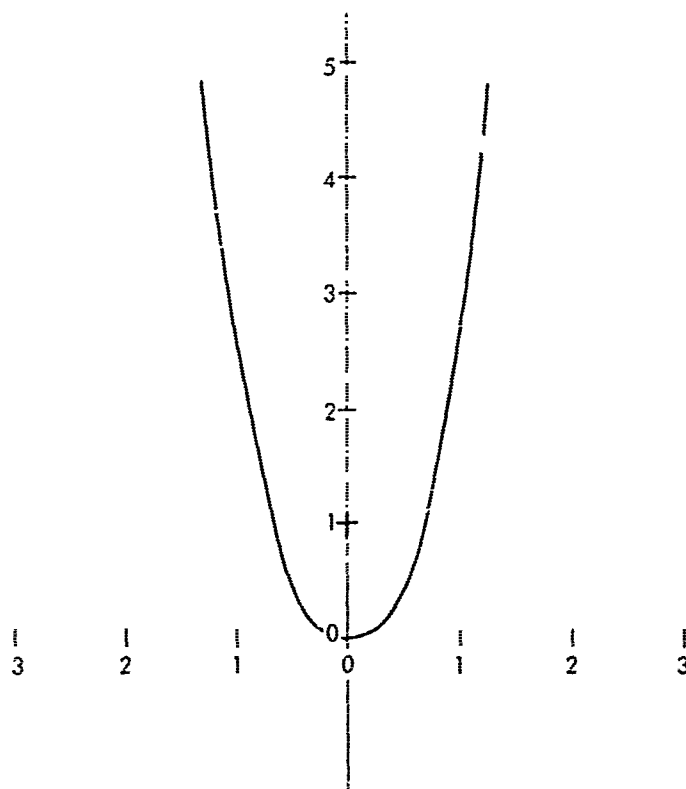


FIG. 2 IDEAL CAVITY DUE TO A 1 1/2-INCH STEEL SPHERE AFTER VERTICAL WATER ENTRY AT 41 FEET PER SECOND FROM AIR AT 1/8TH ATMOSPHERE PRESSURE (DRAWN HALF SIZE)  
AN OBSERVED IDEAL CAVITY DUE TO A 1 1/2-INCH SPHERE ENTERING AT 116 FEET PER SECOND (FIG. 13) CAN BE SUPERIMPOSED ON THIS OUTLINE, FOR COMPARISON

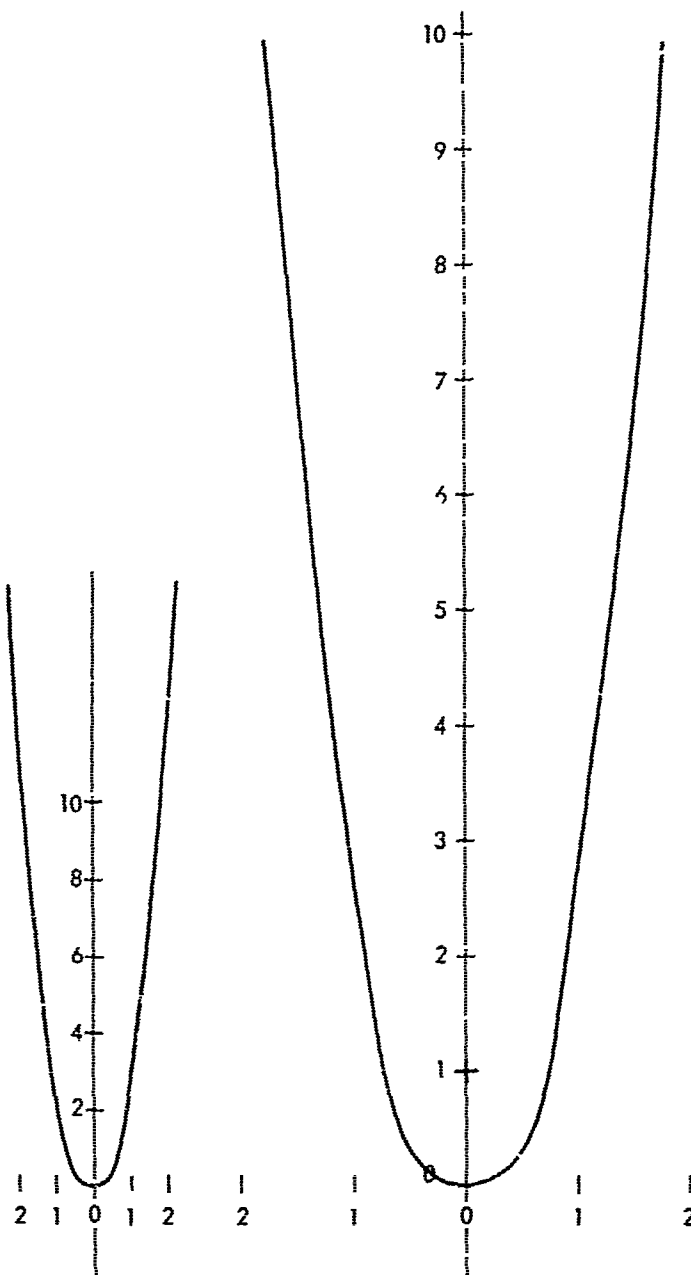


FIG. 10 IDEAL CAVITY DUE TO A 1/2-INCH STEEL SPHERE AFTER VERTICAL WATER ENTRY AT 208 FEET PER SECOND FROM AIR AT 1/28th ATMOSPHERE (DRAWN 1/2 AND 1 1/2 SIZE)

AN OBSERVED IDEAL CAVITY OF A SPHERE (FIG. 13) CAN BE SUPERIMPOSED ON THIS OUTLINE, FOR COMPARISON

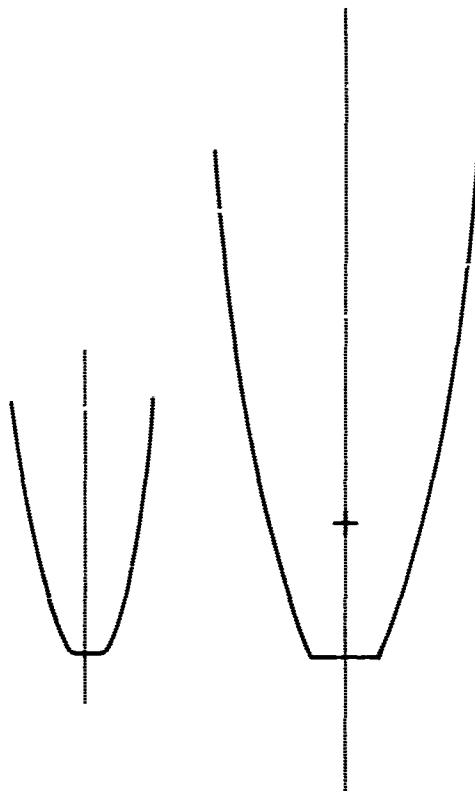


FIG. 11 IDEAL CAVITY DUE TO A 1/4-INCH RIGHT CYLINDER AFTER VERTICAL WATER ENTRY AT 37 FEET PER SECOND. ENLARGED TO APPROXIMATE THE CAVITY OF A RIGHT-CYLINDER WITH THE SAME DRAG AS A 3/4-INCH SPHERE  
AN OBSERVED IDEAL CAVITY OF A SPHERE (FIG. 13) CAN BE SUPERIMPOSED ON THIS OUTLINE, FOR COMPARISON

NOLTR 68-114

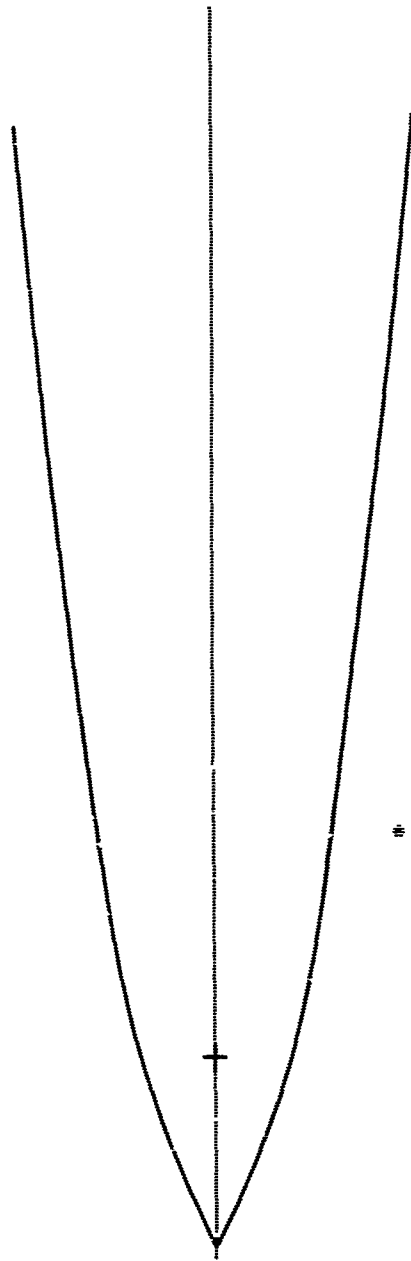


FIG.12 IDEAL CAVITY DUE TO A 45-DEGREE CONE. THE 1 1/2-INCH CONE ENTERED WATER VERTICALLY AT 139 FEET PER SECOND. THE OUTLINE WAS ENLARGED TO APPROXIMATE THE CAVITY OF A CONE WITH THE SAME DRAG AS A 3/4-INCH SPHERE

NOLTR 62-114

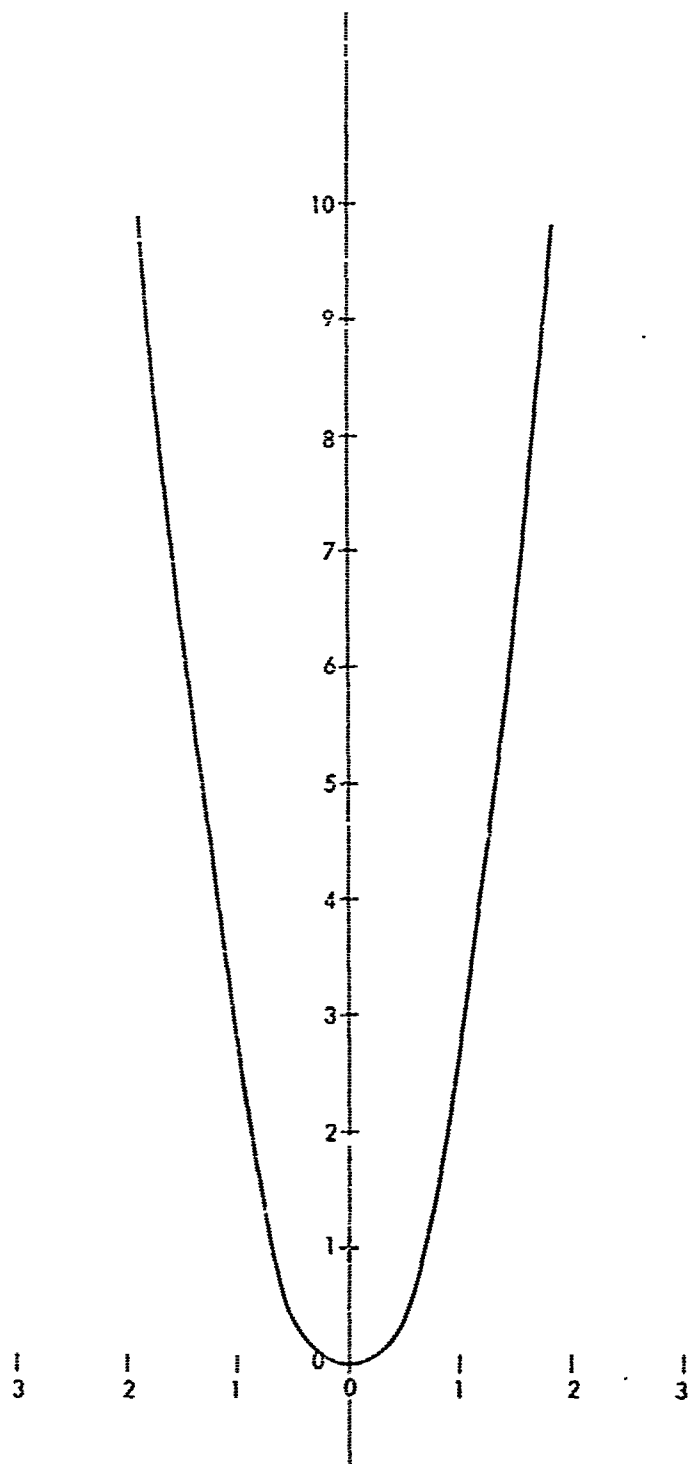


FIG. 13 IDEAL CAVITY DUE TO THE VERTICAL WATER ENTRY OF A 1 1/2-INCH SPHERE AT 116 FEET PER SECOND FROM AIR AT 1/8TH ATMOSPHERE PRESSURE. THIS CAVITY WAS CHOSEN AS A GOOD APPROXIMATION TO THE "IDEAL CAVITY". IT IS DRAWN HALF SIZE. THE PULLOUT SHEET IS SO BOUND THAT IT CAN BE SUPERIMPOSED ON ANY ONE OF THE FIGURES 7 TO 12. THE CAVITY AXES AND THE HEAVY CROSSES SHOULD BE SUPERIMPOSED, FOR BEST AGREEMENT.



FIG.14 LENGTH OF IDEAL CAVITIES FOR RIGHT CYLINDERS WITH DIAMETERS OF 1/4 AND 1/2 INCH.

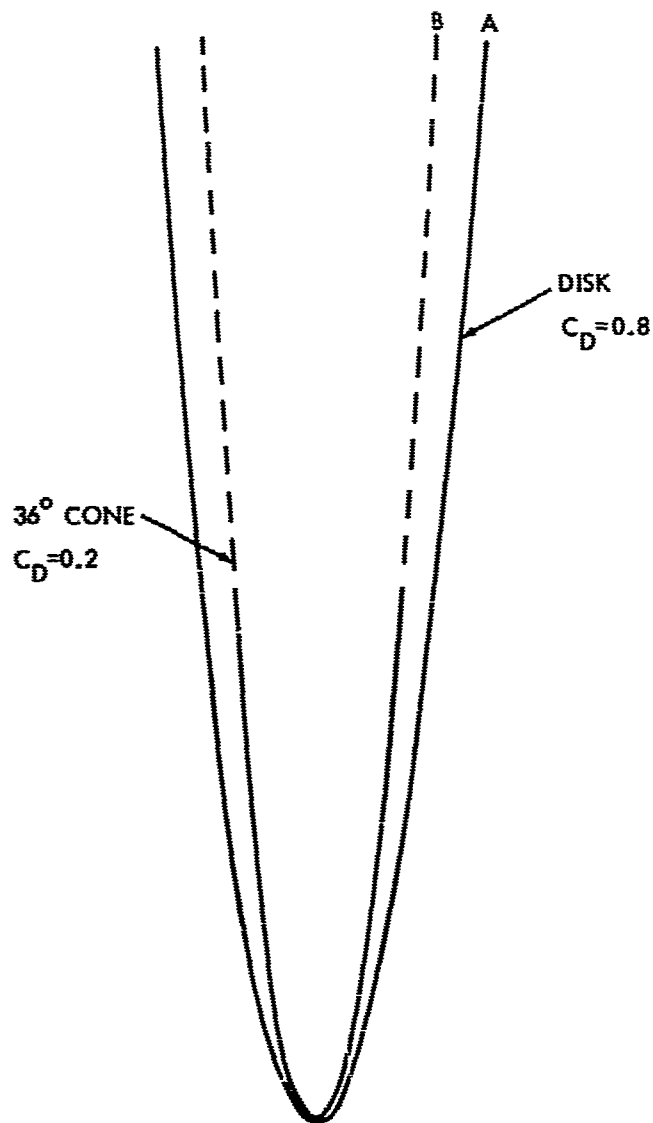


FIG. 15 CALCULATED IDEAL CAVITIES FOR A RIGHT CYLINDER AND A 36-DEGREE CONE OF THE SAME DIAMETER

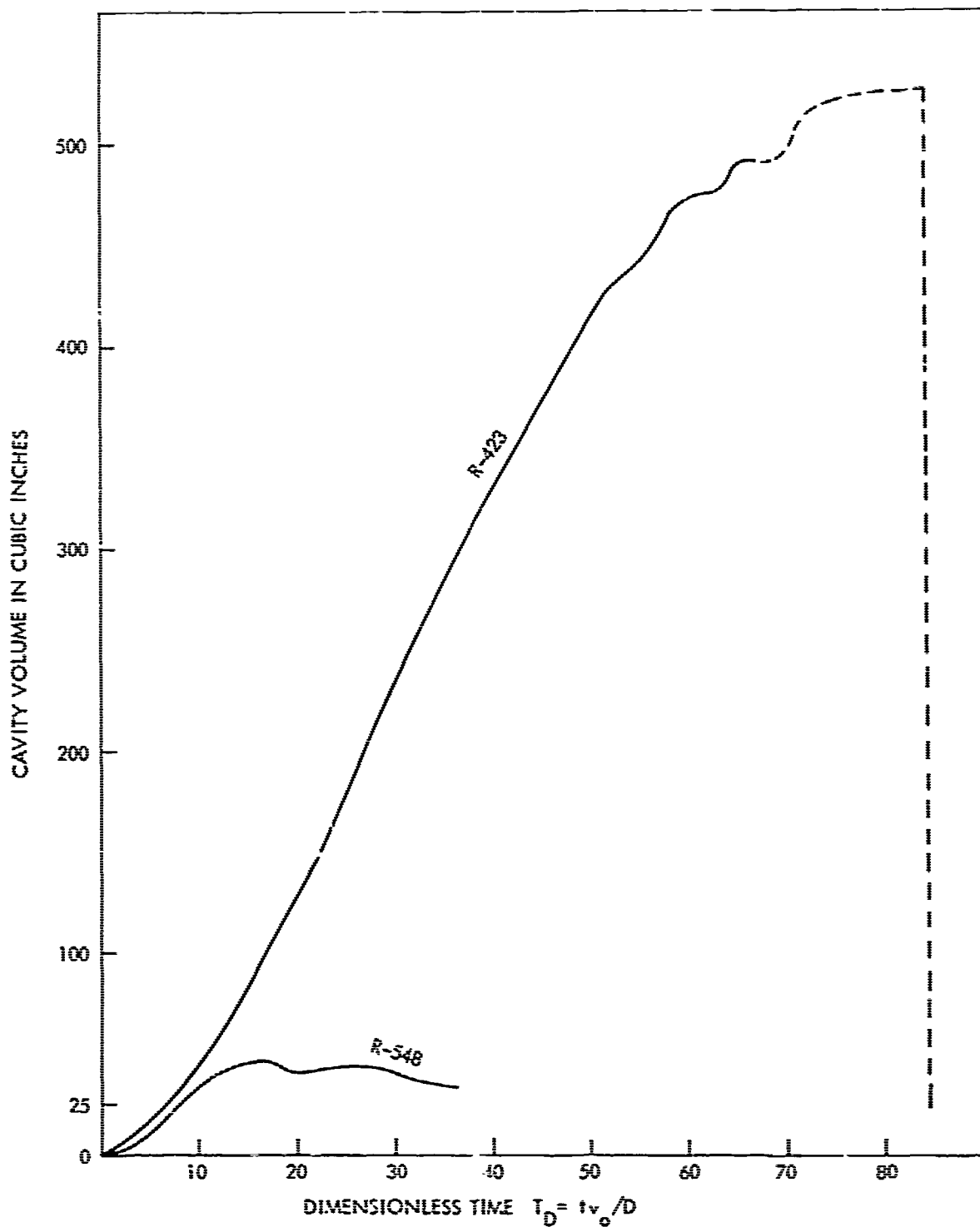


FIG. 16 CAVITY VOLUME WITH AND WITHOUT SURFACE CLOSURE

BOTH VERTICAL WATER ENTRIES WERE OF 1-INCH STEEL SPHERES AT 96 FEET PER SECOND. BECAUSE OF LOW PRESSURE ABOVE THE WATER, ROUND R-423 HAD NO SURFACE CLOSURE. THE VERTICAL LINE SHOWS THE DECREASE IN VOLUME OF THE ATTACHED CAVITY AT DEEP CLOSURE

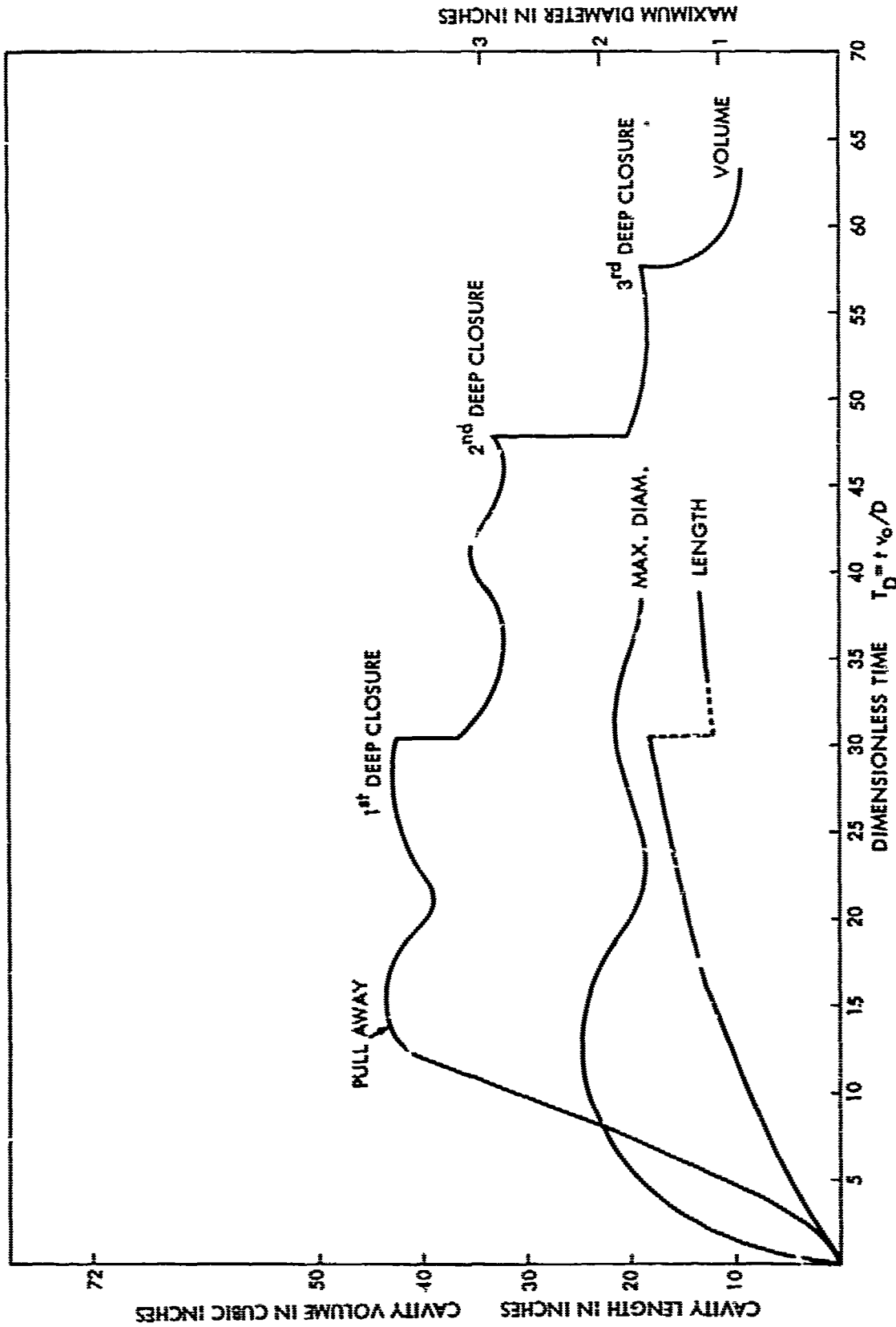


FIG. 17 DEVELOPMENT OF THE CAVITY DUE TO WATER ENTRY OF A SPHERE. THE WATER ENTRY OF A 1-INCH SPHERE WAS VERTICAL AT 96 FEET PER SECOND.

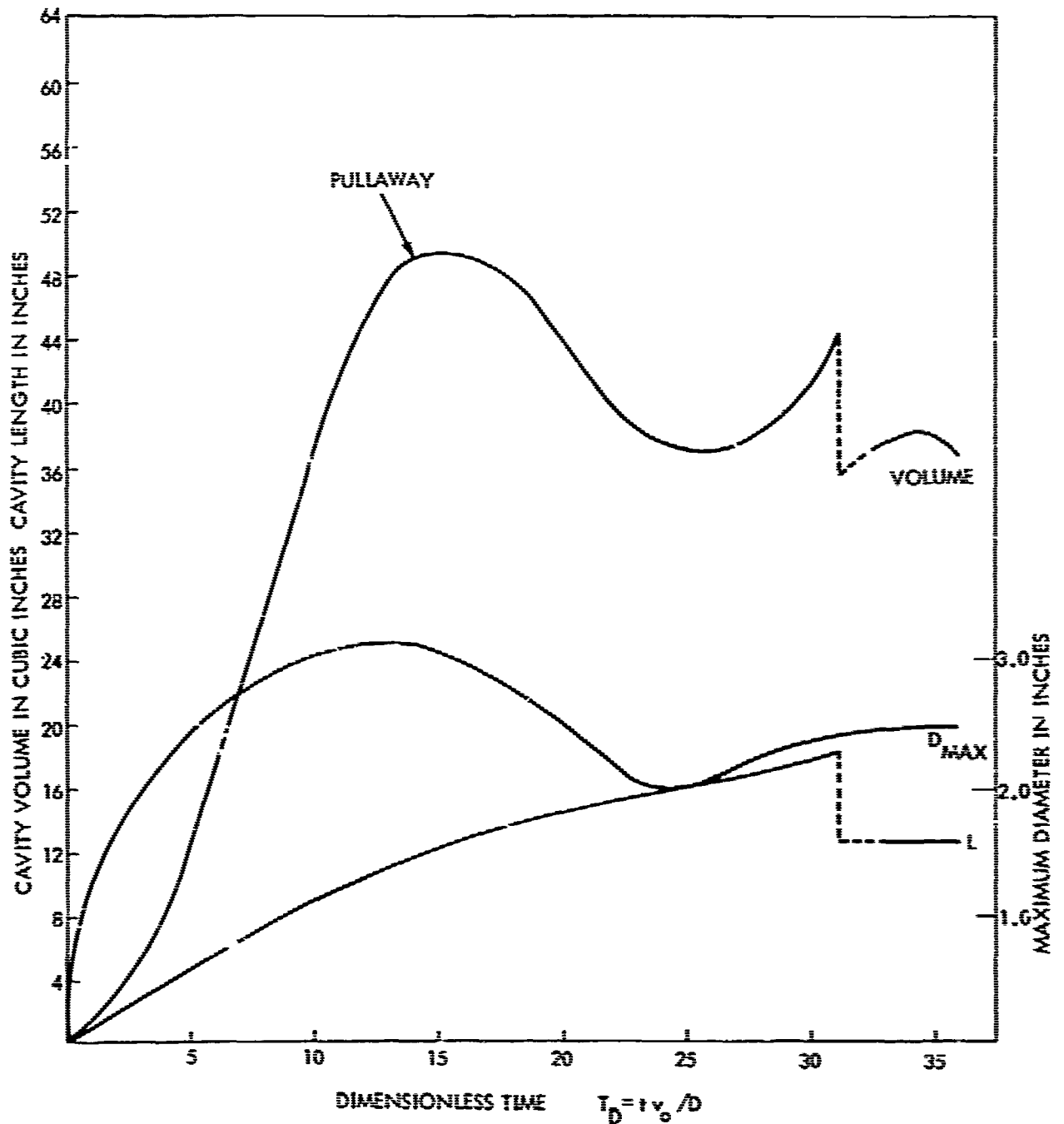


FIG.18 DEVELOPMENT OF THE CAVITY DUE TO WATER ENTRY OF A SPHERE. THE WATER ENTRY OF A 1 1/2-INCH SPHERE WAS VERTICAL AT 125 FEET PER SECOND.

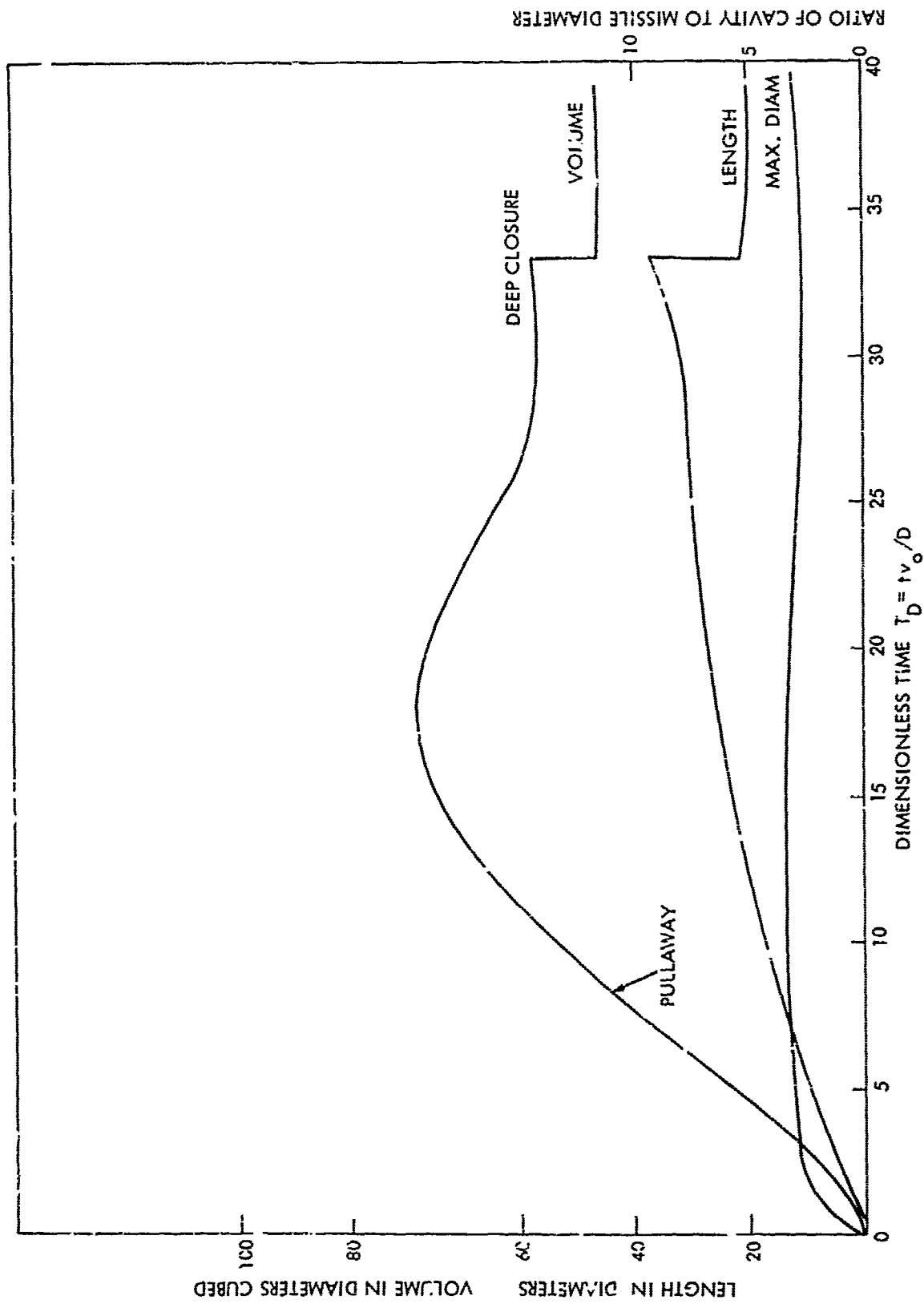


FIG. 19 DEVELOPMENT OF THE CAVITY DUE TO THE WATER ENTRY OF A RIGHT CYLINDER. THIS WAS A VERTICAL ENTRY OF A 1 1/2-INCH RIGHT CYLINDER AT 145 FEET PER SECOND.

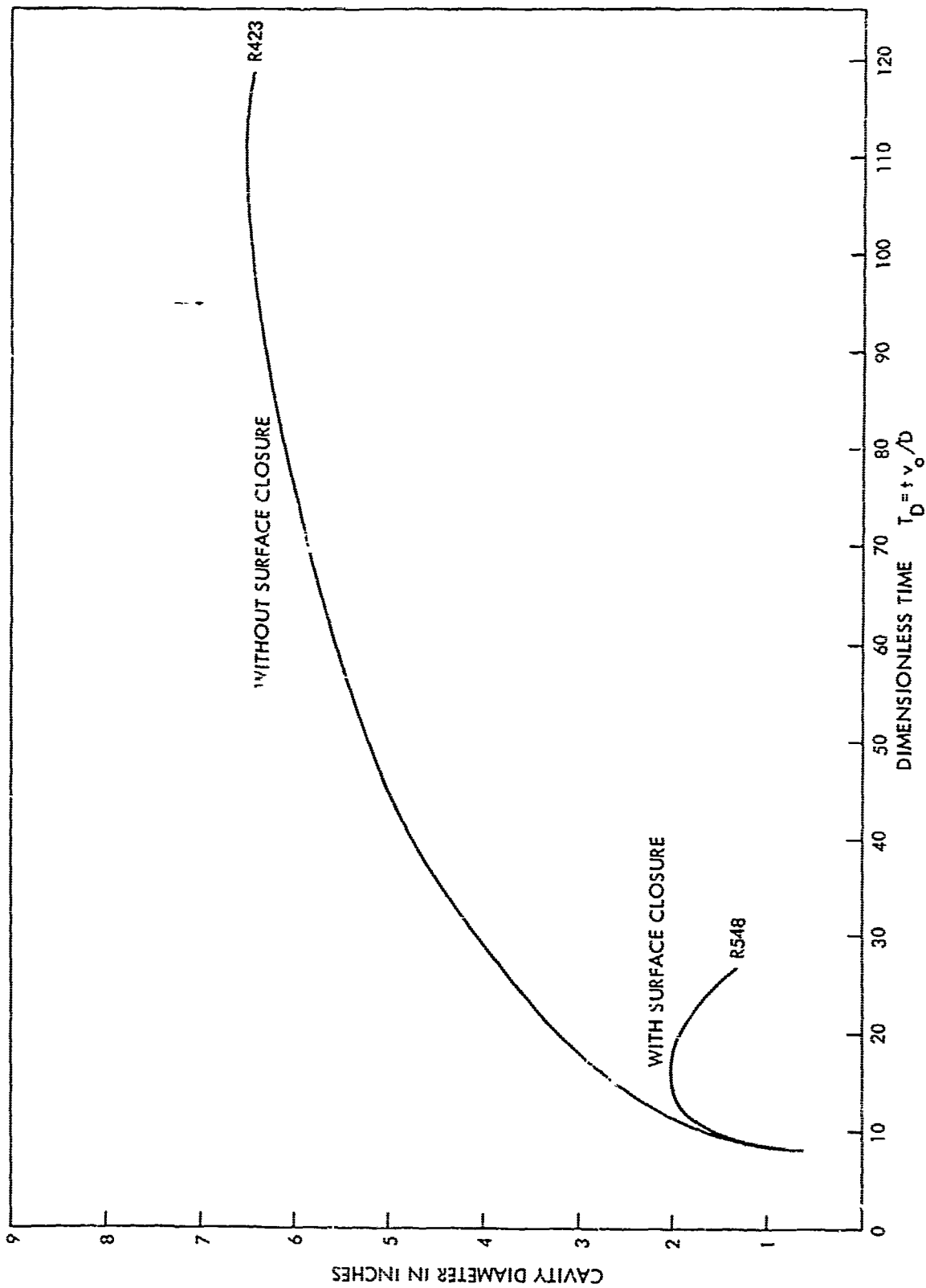


FIG.20 CAVITY DIAMETER WITH AND WITHOUT SURFACE CLOSURE AT A DEPTH OF 7 INCHES  
THESE ARE THE 1-INCH SPHERE ENTRIES WHOSE VOLUMES WERE COMPARED IN  
FIGURE 16.

UNCLASSIFIED

Security Classification

DOCUMENT CONTROL DATA - R & D		
(Security classification of title, body of abstract and indexing annotation must be entered when the overall report is classified)		
1. ORIGINATING ACTIVITY (Corporate author) U. S. Naval Ordnance Laboratory White Oak, Silver Spring, Maryland		2a. REPORT SECURITY CLASSIFICATION UNCLASSIFIED
		2b. GROUP N/A
3. REPORT TITLE THE CAVITY AFTER VERTICAL WATER ENTRY		
4. DESCRIPTIVE NOTES (Type of report and inclusive dates)		
5. AUTHOR(S) (First name, middle initial, last name) Albert May		
6. REPORT DATE 12 July 1968	7a. TOTAL NO. OF PAGES 27	7b. NO. OF REFS 9
8a. CONTRACT OR GRANT NO.	9a. ORIGINATOR'S REPORT NUMBER(S) NOLTR 68-114	
b. PROJECT NO.		
c.	9b. OTHER REPORT NO(S) (Any other numbers that may be assigned this report)	
d.		
10. DISTRIBUTION STATEMENT This document has been approved for public release and sale, its distribution is unlimited.		
11. SUPPLEMENTARY NOTES		12. SPONSORING MILITARY ACTIVITY
13. ABSTRACT At vertical water entry of a missile the splash varies greatly with nose shape and thus modifies the cavity development. Accordingly, the relations reported earlier between cavities formed by different noses at oblique entry, cannot be applied to vertical entry.  An "Ideal Cavity" is defined as that portion of the cavity near the generating nose, which has not been appreciably affected by such influences as gravity or the difference between ambient pressure and the pressure in the cavity. It is shown that all such cavity portions are geometrically similar, with a size proportional to the square root of the drag force, $(C_D A)^{1/2}$ , at a given speed.		

DD FORM 1473 (PAGE 1)

S/N 0101-807-6831

UNCLASSIFIED

Security Classification

UNCLASSIFIED

Security Classification

14.

KEY WORDS

LINK A

LINK B

LINK C

ROLE

WT

ROLE

WT

ROLE

WT

water entry

cavity

UNCLASSIFIED

Security Classification